EurJIC
European Journal of Inorganic Chemistry

A Journal of
ChemPubSoc Europe

Accepted Article

Title: CpRu-complexes containing water soluble phosphine PTA and natural purines adenine, guanine and theophylline: synthesis, characterization and antiproliferative properties

Authors: Lazhar Hajji, Cristobal Saraiba-Bello, Gaspar Segovia-Torrente, Franco Scalambra, and Antonio Manuel Romerosa-Nievas

To be cited as: *Eur. J. Inorg. Chem.* 10.1002/ejic.201900677

Link to VoR: http://dx.doi.org/10.1002/ejic.201900677

WILEY-VCH

CpRu-complexes containing water soluble phosphine PTA and natural purines adenine, guanine and theophylline: synthesis, characterization and antiproliferative properties

Lazhar Hajji,[a] Cristobal Saraiba-Bello,[a] Gaspar Segovia-Torrente,[a] Franco Scalambra,[a] Antonio Romerosa*[a]

Abstract: Complexes [RuCp(Adeninate–κ*N9*)(PTA)$_2$] (**1**), [RuCp(Guaninate–κ*N9*)(PTA)$_2$] (**2**), [RuCp(Theophyllinate–κ*N7*)(PTA)$_2$] (**3**), [RuCp(Adeninate–κ*N9*)(PPh$_3$)(PTA)] (**4**), [RuCp(Guaninate–κ*N9*)(PPh$_3$)(PTA)] (**5**) and [RuCp(Theophyllinate–κ*N7*)(PPh$_3$)(PTA)] (**6**) were synthesized and characterized by NMR spectroscopy, elemental analysis and FT-IR (PTA = 1,3,5-triaza-7-phosphaadamantane). Crystal structures of **1·H$_2$O·3EtOH**, **3·CH$_3$COCH$_3$** and **4·H$_2$O** were also determined by single crystal X-ray diffraction. The antiproliferative activities of the complexes against *cis*platin-sensitive T2 and *cis*platin-resistant SKOV3 cell lines have also been evaluated. Theoretical studies were preformed to elucidate how the adeninate ligand is coordinated to the metal.

Introduction

After the discovery of the anticancer properties of *cis*platin[1] in the sixties by Rosenberg, a huge number of metal derivatives have been synthesized and tested as therapeutic agents for cancer treatment.[2–10] Although the use of *cis*platin and its analogues present important secondary effects,[11–17] they are still some of most widely used chemotherapeutic agents up to date.[18–22] To overcome the drawbacks associated to the platinum drugs, the research on metal complexes bearing different metals is a topic of primary interest.[23–29] Among the non-platinum cytotoxic complexes those containing ruthenium are the most promising.[28,30–36] The Ru(III) complexes NAMI-A[37–40] and KP1019[41–43] entered in clinical trials and in 2011 Dyson *et al.* synthesised the first members of the RAPTA family,[39] which is constituted by Ru(II)-arene complexes containing water soluble phosphanes such as PTA (1,3,5-triaza-7-phosphaadamantane) as hydrophile ligand. The members of this family showed to be particularly effective against platinum resistant cancer cells. The excellent antiproliferative activity showed by RAPTA complexes have deeply pushed their study [39,40,44–47] and have spread the use of PTA and its derivatives as ligands in cytotoxic metal complexes, which has been recently reviewed.[48–51] These type of ligands have been showed to be useful also to obtain Ru(II)-bipyridine[52] and Ru(II) piano-stool complexes with interesting antiproliferative profiles.

The design of antiproliferative metal complexes requires, additionally to an active metal, the adequate combination of appropriate ligands that modulate both the activity and the partition coefficient of the complex. The latter has been found to be a factor of main importance to increase the cytotoxicity: the complex has to solubilize in both the water-rich plasma and the hydrophobic cell membrane.[53]

Ligands PTA, mPTA (N-methyl-1,3,5-triaza-7-phosphaadamantane) and its derivative dmoPTA (3,7-dimethyl-1,3,7-triaza-5-phosphabicyclo[3.3.1] nonane) have an adequate hydrophilic/hydrophobic balance to move through the biological system, which most of the times does not vary after coordination to metals. We obtained promising results with platinum[54,55] and ruthenium[56] complexes containing the water soluble phosphine PTA and its derivative mPTA and noteworthy also with dmoPTA,[56–64] which showed to be an excellent ligand to synthesise ruthenium complexes active against *cis*platin sensitive and resistant cell lines.

It was showed that the binding of a ruthenium complex to natural purines could enhance the antiproliferative activity of both species by a synergic action and could affect the metal distribution in the cells by a ligand "carrier effect". In the last years we also noticed that the introduction of a purine in the coordination sphere of piano-stool ruthenium complexes could enhance their antiproliferative activity. This was corroborated synthesising the ruthenium complexes [RuCp(X)(PTA)(L)] (X = 8-thio-theophyllinate, 8-methylthio-theophyllinate, 8-benzylthio-theophyllinate; L = PTA, PPh$_3$) containing thiopurines. It was showed that the antiproliferative activity of these complexes against T2 (*cis*platin-sensitive) and SKOV3 (*cis*platin-resistant) cell lines was enhanced with respect to the starting compounds,[65] and to similar ruthenium complexes containing PTA or mPTA, but without the purine.[66]

In this work we extend the study of the reactivity of [RuClCp(PTA)(L)] (L = PTA, PPh$_3$) type complexes to the natural purines adenine, guanine and theophylline. The latter has been chosen due to the lack of the N10 coordination site, that simplifies its coordination chemistry, helping also the NMR characterization of the reaction products with adenine and

[a] Área de Química Inorgánica-CIESOL
Universidad de Almería
Carretera Sacramento s/n 40120 Almería, Spain
E-mail: lazharhajji1000@gmail.com
saraiba@ual.es
gfst75@gmail.com
fs649@inlumine.ual.es
romerosa@ual.es
http://cvirtual.ual.es/webual/jsp/investigacion/nuevo/pInicio.jsp?id_grupo=FQM317&idioma=es

ORCID(s) from the author(s) for this article is/are available on the WWW under

guanine by comparison. Interestingly the obtained results showed that adenine and guanine are coordinated by the imidazolic N9 atom, while theophylline by the N7. The resulting complexes [RuCp(X)(PTA)(L)] (X = κ*N9*-adeninate, κ*N9*-guaninate, κ*N7*-theophyllinate; L = PTA, PPh_3) showed different partition coefficient and antiproliferative activity. A theoretical study on the ruthenium complexes with adeninate and guaninate was also performed with the aim to determine the reasons why purine is coordinated to the metal by the imidazolic N9 atom.

Results and Discussion

Reactivity of [RuClCp(PTA)$_2$] with adenine, guanine and theophylline: synthesis and characterization of 1-3.

Complex [RuClCp(PTA)$_2$] was initially reacted with adenine, guanine or theophylline in water and in a mixture of water/EtOH at room and refluxing temperature. In these conditions no reaction occurred but when the purines were previously deprotonated the corresponding purinate substituted the chloride in the starting complex. The complexes **1**-**3** (adeninate for **1**, guaninate for **2** and theophyllinate for **3**) were obtained in good yield in refluxing EtOH/water by reaction of [RuClCp(PTA)$_2$] with the resultant purinate of prepared by deprotonation of the purine with KOH in EtOH (Scheme 1). It is important to point out that all of the obtained compounds are stable in solid state for months under air at room temperature, and in water solution for more than 2 days, even when DMSO-d_6 (from 10 to 50% v/v) was introduced in the solution and the temperature kept at 40 ºC. Also, complexes were stable for 1 day at room temperature and 40 ºC in a DMSO-d_6/cellular-culture dissolution.

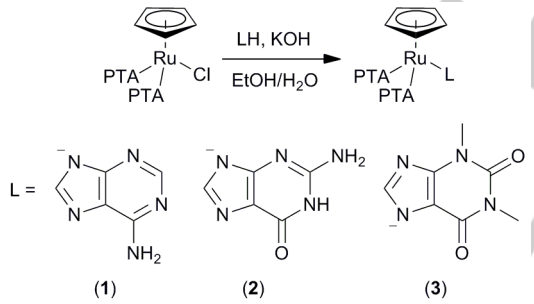

Scheme 1. Synthesis of **1**-**3**.

The $^{31}P\{^1H\}$ NMR of **1** showed a singlet at -23.17 ppm, that is similar to that observed for the starting complex [RuClCp(PTA)$_2$] (-25.65 ppm) and corresponds to the PTA ligands.[67] The presence of the adeninate in **1** is evidenced by the characteristic IR strong absorption bands for δ(NH_2) (1629, 1594 cm-1) and ν(C=C+C=N) (1542 cm-1). The ^1H NMR spectrum of **1** in D_2O displays singlets at 7.66 ppm and 8.21 ppm integrating 1 H, ascribable to adeninate-C2-H and C8-H respectively.[68–70] Unfortunately the complexes are not soluble enough in any aprotic solvent for observing the adeninate-NH_2. The characteristic signals for Cp and PTA for a piano-stool structure were observed, supporting that the complex retains the same ligand configuration with respect to the starting complex. The Cp and PTA signals in the $^{13}C\{^1H\}$ NMR spectrum also agree with the proposed structure for **1**, the rest of the spectrum does not deserve particular comments.

Despite of the N7 imidazolic atom is the most popular coordination position for adenine with transition metals, at the best of our knowledge this is the first example characterized by single crystal X-ray diffraction of an adeninate-ruthenium complex mono-coordinated by N9.[71] Therefore, although in **1** the most probable coordination of the adeninate to the ruthenium is the imidazolic N9, the spectroscopic evidences are not enough for ensuring this suspicion. Fortunately, crystals good enough for single crystal X-ray diffraction were obtained and the structure for **1** was fully determined (Figure 1). As expected the ruthenium is coordinated to a η^5-Cp, to two PTA by the P atoms and to an adeninate by the N9.

The elemental analysis, IR and NMR spectroscopy also supported that complex **2** is constituted by a ruthenium coordinated to a η^5-Cp, two P_{PTA} by the P atoms and a guaninate ligand, but newly these techniques do not provide evidences to propose which is the coordination site of the guaninate.[71]

Complex **3** was fully characterized by spectroscopic techniques. Its IR spectrum, ^1H and $^{13}C\{^1H\}$ NMR spectra showed that the theophylline is coordinated by the imidazolic N7 atom, such as was observed in a large amount of similar Cp-PTA-ruthenium examples containing thiotheophyllines, some of them fully characterized by single crystal X-ray diffraction.[58]

Reactivity of [RuClCp(PPh_3)(PTA)] against adenine, guanine and theophylline: synthesis and characterization of complexes 4-6

Similarly to what described previously for the reactivity of [RuClCp(PTA)$_2$], neither the starting complex [RuClCp(PPh_3)(PTA)] reacts with adenine, guanine and theophylline at room and refluxing temperature. Nevertheless, when purines were deprotonated, they substitute easily the chloride in the starting complex. The respective purinate was reacted with the starting complex [RuClCp(PPh_3)(PTA)] (Scheme 2), affording quantitatively complexes **4**-**6** (**4**: adeninate; **5**: guaninate; **6**: theophyllinate). All of these complexes are not

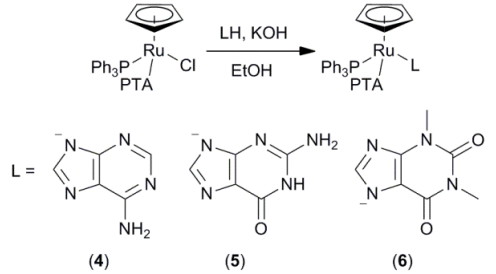

Scheme 2. Synthesis of **4**-**6**.

soluble in water but in organic solvents such as $CDCl_3$, in which they are stable for more than 2 days also when DMSO-d_6 is added (from 10 to 50% v/v) at room temperature and at 40 ºC. In the solid state they are stable for months at room temperature under both N_2 and air.

The IR spectrum of complex **4** showed characteristic $\delta(NH_2)$ absorption bands (1623, 1593 cm^{-1}) and ν(C=C + C=N) (1541 cm^{-1}) in the typical range found for an adeninate ligand coordinated to ruthenium.[68–70] This evidence was also supported by the ^1H and ^{13}C NMR spectra. In complex **4** the ruthenium is coordinated to four different ligands and therefore the metal is a chiral center (Scheme 2). The ^1H NMR ($CDCl_3$) displayed the expected sharp signals for one Cp, one PTA and one PPh_3 ligand as well as signals for the NH_2 (5.42 ppm), C2-H (7.71 ppm) and C8-H (8.34 ppm) of adeninate protons. The $^{13}C\{^1H\}$ NMR of **4** presents the expected signals for its proposed composition. Interestingly, the $^{31}P\{^1H\}$ NMR spectrum showed the expected two doublets at 52.12 ppm (PPh_3) and -35.74 ppm (PTA), somewhat shifted with respect to those of the starting complex [RuClCp(PPh_3)(PTA)] (δ PPh_3 = 48.16 ppm; δ PTA = -34.96 ppm). These signals arise also at a different chemical shift to that found for the monometallic complexes containing thiopurinate ligands.[65] Again, looking at the spectroscopic data, it is not possible to guarantee which is the adeninate coordination site. The crystal structure of **4** was determined by single crystal X-ray diffraction (Figure 1) that shows how the ruthenium is coordinated with a piano-stool geometry to a η^5-Cp, a PTA and a PPh_3 by their P atoms and to the imidazolic N9 atom of an adenine molecule.

The complex **5** was synthesized by a procedure similar to that for **4** and therefore a similar complex was expected but containing guaninate instead of adeninate. The IR spectrum of **5** showed the typical bands for coordinated guaninate ($\delta(NH_2)$=1672 (s); ν(C=O)=1608 (s); ν(C=C+C=N)=1564 (m)),[72–74] and its ^1H NMR spectrum displays the characteristic signals for PPh_3, PTA and Cp in a piano-stool configuration.[65] The guaninate signals arise at 5.86 ppm (NH_2) and 7.14 ppm (C8-H), which are similar to those found for **2** (δ(C8-H) = 7.35 ppm). In this complex the $^{13}C\{^1H\}$ NMR spectrum displays sharp peaks for Cp, PTA and PPh_3 carbon atoms but broad signals for guaninate carbons, arising at chemical shifts (C5: 118.58 ppm; C8: 151.15 ppm; C4: 153.78 ppm; C2: 157.68 ppm; C6: 162.93 ppm) similar to those found in **2** (C5: 116.60 ppm; C8: 151.37 ppm; C4: 154.32 ppm; C2: 159.08 ppm; C6: 163.15 ppm). Therefore, it is reasonable that in both complexes the purinate is coordinated by the same coordination position. Finally, the $^{31}P\{^1H\}$ NMR spectrum of **5** is constituted by two doublets with similar chemical shift and coupling constant with respect to **4**.

The IR absorption bands of **6** arise at similar frequency than those found in similar theophyllinate ruthenium complexes,[75–77] which suggests that purine is coordinated to the metal by the imidazolic N7 atom. The ^1H NMR spectrum shows the signals expected for a metal coordinated to a η^5-Cp, a PPh_3, a PTA and the theophyllinate. The ^1H NMR spectrum of complex **6** displays broad signals. As indicated previously, the ruthenium atom is a chiral center and therefore different isomers can be obtained from the synthesis. The ^1H, $^{13}C\{^1H\}$ and $^{31}P\{^1H\}$ NMR of **6** are similar to complex [RuCp(thiopurinate)(PPh_3)(PTA)] in which was also evident the presence of different isomers in solution.[56,65] Similarly to **4** and **5**, the possible isomers constituting **6** were not isolated.

Crystal structures of [RuCp(Adeninate–κN9)(PTA)$_2$]·H_2O·3EtOH (1·H_2O·3EtOH), [RuCp(Theophyllinate-κN7)(PTA)$_2$]·(CH_3COCH_3) (3·CH_3COCH_3) and [RuCp(Adeninate–κN9)(PPh_3)(PTA)]·H_2O (4·H_2O)

Single crystals of **(1·H_2O·3EtOH)** and **(4·H_2O)** grew by slow evaporation of an ethanol/water solution containing the respective complex. The asymmetric units are constituted by a molecule of neutral complex [RuCp(Adeninate–κ*N9*)(PTA)$_2$] (**1**) or [RuCp(Adeninate-κ*N9*)(PPh_3)(PTA)] (**4**), plus crystallization solvent (water and/or ethanol). The complex units are typical piano stool η^5-Cp moieties containing two PTA (**1**) or a PTA and a PPh_3 (**4**). In both the cases the coordination sphere of the ruthenium is completed by an adeninate coordinated by its N9 (Figure 1). At the best of our knowledge they represent the first example of monometallic Ru-adeninate complexes where the adeninate is coordinated to the ruthenium via N9 instead of the most accessible NH_2. Up to date, the reported Ru-adenine complexes[68–70] are coordinated by N7/N9 (the polymetallic tetrakis((μ_2-Adeninate-N^7,N^9)-(η^6-benzene)-chloro-ruthenium)tetrachloride-decahydrate)[78] and N7/NH_2/N1 (Cyclo-(tetrakis((μ_2-Adeninate)-(η^6-p-cymene)-ruthenium)tetrakis-trifluoromethylsulfonate)[79,80] but there is not any crystallographycally characterized example in which an adenine molecule is mono-coordinated to a ruthenium atom through N9.

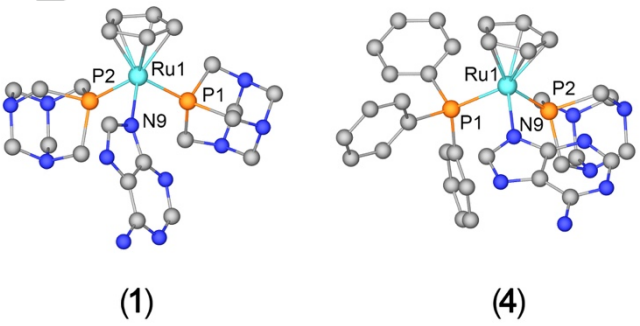

Figure 1. Representations of the crystal structure of **1** and **4**. For the sake of clarity the H atoms were omitted.

The distances between the metal and the PTA or the PPh_3, are in the expected range (**1**: Ru-P1 = 2.2834(9) Å, Ru-P2 = 2.2556(6) Å; **4**: Ru-P1 = 2.304(2) Å, Ru-P2 = 2.304(2) Å).[56,65] In complex **4** the Ru-P distances are identical, while in complex **1** they are slightly different between each other, that was not observed in the starting complex [RuClCp(PTA)$_2$] (Ru-P1 = 2.258 Å, Ru-P2 = 2.247 Å). The Ru-$Cp_{centroid}$ bond lengths are also similar to those of other similar piano-stool ruthenium complexes containing PTA or mPTA (**1**: 1.860Å; **4**: 1.855 Å).[56]

The Ru-N9 distances (**1**: 2.146(2) Å; **4**: 2.142(7) Å) are comparable to those found in a polymetallic N7/N9-adeninate ruthenium complex (2.117(10) Å)[78] and in a N7/NH_2/N9-adeninate cyclo-ruthenium complex (Ru-N9 = 2.079(4) Å).[79,80] For what concern **1**, the purine plane is located between both PTA molecules, while in **4** it is almost parallel to the Cp ring, probably to minimize the steric hindrance. The distances C8-N9 (**1**: 1.363(4) Å; **4**: 1.291(11) Å) and C8-N7 (**1**: 1.328(3) Å; **4**: 1.349(11) Å) indicate that the single bond character of C8-N9 and the double bond character of C8-N7 bond are higher in complex **4** (**1**: Δ = 0.035(2) Å; **4**: Δ= 0.058(11) Å). In both cases, the bond character is quite different than those found in N7-N9 bridged Ru-adeninate complexes, such as complex [{RuCl(μ_2-adeninate-N^7,N^9)(η^6-p-cymene)}$_4$]$^{4+}$ (N9-C8 = 1.329(4) Å; C8-N7 = 1.335(4) Å; Δ = 0.006(4) Å).[78] This fact supports the single character for the bond between N9 and C8 while that between N7-C8 is close to double and agrees with complex *trans*-[Pd-(adeninate)$_2$(n-$Bu_3P)_2$],[81] in which the adeninate is bonded to the metal by only N9, the distances N9-C8 and C8-N7 (N9-C8 = 1.359(5) Å; C8-N7 = 1.319(5) Å), are practically the same of those in **1** and **4**, but also in Ni, Pt and Zn complexes containing the monodentate N9-coordinated-adeninate ligand.[82–84] The rest of the distances in the adeninate ligand in **1** and **4** are similar to those found in known Ru-adeninate complexes.[78–80] The angles around the ruthenium in **1** (P1-Ru-P2 = 96.01(3)º, P1-Ru-N9 = 96.06(7)º, P2-Ru1-N9 = 88.17(7)º) and **4** (P1-Ru-P2 = 95.96(7), P1-Ru-N9 = 95.48(18)º, P2-Ru1-N9 = 90.75(19)º) are approximately 1 - 5º wider than those in the respective starting complexes, presumably due to the steric hindrance imposed by the adeninate. In the packing of both **1·H_2O·3EtOH** and **4·H_2O**, the complex units are dimerized through a network of hydrogen bonds involving the water or ethanol solvate and the non coordinated nitrogens of the adeninate ligand.

For what concern **3·CH_3COCH_3**, single crystal were obtained by evaporation of an acetone solution of **3**. It is the first example of a ruthenium complex containing theophylline determined by single crystal X-ray diffraction, according to CCDC.[71] A representation of the complex structure is displayed in Figure 2, the crystallographic data are showed in Table 1 and a list of selected bond distances and angles in Table 2. The asymmetric unit contains one [RuCp(theophyllinate-κ*N7*)(PTA)$_2$] complex and one acetone molecule. The complex unit is constituted by a distorted piano-stool octahedral ruthenium coordinated to a η^5-Cp, two PTA via *κP* and a theophylline by the imidazolic N7 atom. The Ru-P and Ru-N are similar to **1** and **4** and agree with what found for similar complexes (Ru-P1 = 2.271(1) Å, Ru-P2 = 2.267(1) Å, Ru-N1 = 2.142(4) Å).[56,65][85] The purinate plane is almost parallel to the Cp ring, as observed in **4**. The distances C8-N7 (1.339(6) Å) and C8-N9 (1.346(6) Å) are similar to each other, while the C5-N7 bond length is somewhat longer (1.409(6) Å), which agrees well with theophyllinate complexes of Cu,[86] Au,[70] Cd,[87] Hg,[88,89] Co[90] and Zn.[91] The angle between PTA ligands (P1-Ru-P2 = 93.06(4)º) is shorter than in **1** and **4**, and it is nearly bisected by the Ru-N7 bond (P1-Ru-N7 = 93.37(10)º, P2-Ru-N9 = 93.37(10)º).

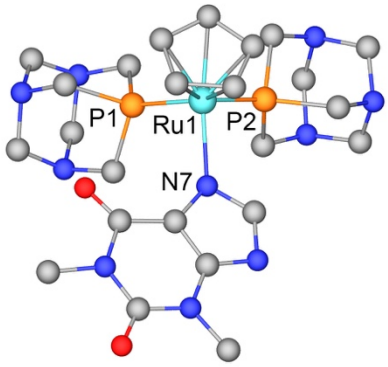

Figure 2. Representation of the crystal structure of **3**.

Table 2. Selected bond lengths and angles for **1**, **3** and **4**.

	1	**3**	**4**
	Bond length (Å)		
Ru1-P1	2.2834(9)	2.271(1)	2.304(2)
Ru1-P2	2.2556(6)	2.267(1)	2.304(2)
Ru1-N7	-	2.142(4)	-
Ru1-N9	2.146(2)	-	2.142(7)
N7-C5	1.372(4)	1.409(6)	1.389(11)
N7-C8	1.328(3)	1.339(6)	1.349(11)
N9-C4	1.364(3)	1.354(6)	1.388(9)
N9-C8	1.363(4)	1.346(6)	1.291(11
C4-C5	1.394(4)	1.377(6)	1.406(11)
	Angle (º)		
P1-Ru1-P2	96.01(3)	93.06(4)	95.95(7)
P1-Ru1-N7	-	93.37(10)	-
P1-Ru1-N9	96.06(7)	-	95.48(18)
P2-Ru1-N7	-	93.35(10)	-
P2-Ru1-N9	88.17(7)	-	90.75(19)

Theoretical calculations

In order to shed light on why Ru is coordinated to the imidazolic N9 atom instead of the N7, bond energies and bond orders were calculated for complexes **1, 4** and their N7-coordinated analogues **1a**, **4a and 4b** (Figure S21). For complexes **1** and **4** the calculated Ru-N9 bond length was similar to that in crystal structure (differences < 1%).

Complex **1** is 12.8 kcal/mol more stable than its N7 isomer **1a** (Figure S21). For what concern **4**, two different disposition of the adeninate where considered for the N7: the adeninate-NH_2

pointing to the PTA (**4a**) or to the PPh_3 (**4b**). These complexes showed to be even less stable than **4** but also than **1b** (**4**-**4a**: 14.2 kcal/mol**;** **4**-**4b**: 15.5 kcal/mol). The dissociation energy of the $\{RuCp(L_2)\}^+$ moiety from the adeninate ligand is higher if the ligand is coordinated by the imidazolic N7 atom (**1**-**1a**: 13.2 Kcal/mol; **4**-**4a**: 23.2 kcal/mol**;** **4**-**4b**: 24.5 kcal/mol), therefore these results support that the Ru-N9 bond is stronger that the Ru-N7. These results evidence not only that **1** and **4** are more stable than **1a** and **4a/b**, respectively, but also that the energy gap between Ru-N7 and Ru-N9 isomers increases when a PTA is replaced with a bulkier triphenylphosphine. This suggests that the adeninate-N7 coordination could be less favored than the N9 due to the steric hindrance imposed by the adeninate-NH_2 group and the bulky PPh_3.

Cell Growth Inhibition

There are significant examples on how the antiproliferative activity of metal complexes is amplified when they are reacted with biologically active molecules and in particular with natural purines. With this idea in mind, the cell growth inhibition activities of complexes **1**-**6** were evaluated.

Complexes **1**-**3** and **4**-**6** have been tested for cell growth inhibition activity on the *cis*platin-sensitive human cancer cell lines T2 and on the *cis*platin-resistant SKOV3 and compared with the starting complexes $[RuClCp(PTA)_2]$ and $[RuClCp(PPh_3)(PTA)]$ (results reported in Table 3). Despite of the growth inhibition activity for *cis*platin and starting compounds were previously published,[56] they were also checked in the same experiment for the sake of comparison. The general standard procedure consist in dissolving the complex in DMSO and quick addition of AIM-V medium to obtain solutions of 50, 10 and 2 μM. The percentage of growth inhibition at the three doses for each complex allowed us to estimate the IC50, the concentration reducing to 50% the cell growth of both cell lines. Complexes **1**-**6** are stable under air in solid state for months and in water and in a mixture of water/DMSO under air at both room temperature and 40 ºC for 2 days.

Tests with the *cis*platin-sensitive cells T2 showed that complex **4** displays a significantly better activity than the others. The antiproliferative activities of related PTA Ru[56,65] and Pt[55] complexes were correlated with their solubility in lipophilic media, which is connected with the ability of the compound to cross the lipophilic membranes of the cell. If the antiproliferative action mechanism involves the reaction of the compound with internal components of the cell, only those complexes capable of crossing membranes can react with internal cell components. Partition coefficients, Log *P*, for complexes (Table 3) show as the complexes **4**-**6**, containing PTA and PPh_3, are more lipophilic (positive Log *P*) than **1**-**3**, which bear two PTA. Nevertheless, despite complex **4** shows both the largest antiproliferative activity and Log *P*, supporting the initial idea than the antiproliferative activity is related with the partition coefficient, complex **5**, which displays the second larger partition coefficient, does not show significant antiproliferative activity.

For the sake of looking for some other parameters that could determine the observed antiproliferative activity, the water solubility and the oxidation potential of the complexes were taken in account (Table 3). More data are needed to ensure a tendency but from the results obtained complex **4**, which show the largest antiproliferative activity, also display the largest water solubility and oxidation potential. Complex **4** displays the highest activity against T2 cell line, better than that for *cis*platin. Tests with the *cis*platin-resistant SKOV3 cell line showed that this complex is also more active than *cis*platin on Pt-resistant cell line. This observation supports the hypothesis that complex **4**, which is as active as *cis*platin on Pt-sensitive cells and also more active than *cis*platin on Pt resistant cell line, could act by a different mechanism than the classical Pt containing drugs. Despite of all of the available Ru coordination sites are filled, the ligands could be substituted by a nucleophile inside the cell such as a DNA-purine, similarly to Cl in cisplatin is substituted first by H_2O and finally for DNA-guanine. Nevertheless, and taking in account the observed stability of the complexes in DMSO-d_6 and DMSO-d_6/cell-culture-medium, an alternative to this hypothesis could be formation of the strong hydrogen bonds between DNA purine bases and the adenine in **4** as it was observed between adenines of neighbors molecules in the crystal structure. Although this possibility is intriguing, a large and intense research work needs to be done to determine if this effect could determine the antiproliferative activity of **4**.

Table 3. Estimated IC50 on *cis*platin sensitive T2 cell line and *cis*platin-resistant SKOV3 of complexes **1**-**6**, Log *P*, S_{25,H_2O} and E_o.

Complex	IC50 (μM)		Log *P*	S_{25,H_2O} (mg/cm^3)	E_o (V)
	T2	SKOV3			
$[RuClCp(PTA)_2]$	> 50	> 50	-1.85		
1	>50	> 50	-0.82	15.8	0.620
2	> 50	> 50	-1.19	3.5	0.974
3	>50	> 50	-0.45	14	0.684
$[RuClCp(PPh_3)(PTA)]$	10-50	> 50	0.75		
4	<2	30±20	1.4	0.6	0.690
5	>50	> 50	1.32	0.4	0.407
6	ca 50	ca 50	0.81	0.8	0.726
*cis*platin	6±4	> 50			

Conclusions

The reactivity of starting complexes with antiproliferative activity $[RuClCp(PTA)_2]$ and $[RuClCp(PPh_3)(PTA)]$ against natural purines adenine, guanine and theophylline showed that reaction proceed when purine is previously deprotonated. The six new Ru(II) complexes obtained display a similar structure constituted by a octahedral piano-stool Ru bonded to a η^5-Cp, to two

phosphines by the P atoms and the natural purinate (**1**-**3**: containing two PTA; **4**-**6**: containing a PTA and a PPh_3). The antiproliferative activities of complexes **1**-**6** were evaluated on model tumoral cell lines T2 and SKOV3. Only complex **4** ([RuCp(Adeninate–κ*N7*)(PPh_3)(PTA)]), showed similar activity to *cis*platin on T2 cell line but better than *cis*platin on SKOV3 cell line. The valuable anticancer activity of **4** is probably due to a convenient hydrophilicity/lipophilicity balance reached upon combination of the ligands, associating one hydrophilic PTA with the lipophilic PPh_3 and the adenine, but also its oxidation potential could have some substantial influence.

It is captivating to consider that the real reason that can justify the antiproliferative activity of **4** is its capability of forming strong hydrogen bonds through the adenine-atoms with the DNA-purine bases, making the interaction mechanism different than that for starting complex. A large work is needed to support this idea, but for sure, the piano-stool ruthenium complexes could improve its antiproliferative activity including in its composition natural purine.

Experimental Section

General Procedures. All chemicals were reagent grade and were used as received by commercial suppliers unless otherwise stated. The solvents were all degassed and distilled according to standard procedures.[92] All reactions and manipulations were routinely performed under a dry nitrogen atmosphere by using standard Schlenk-tube techniques. The compounds PTA, [RuClCp(PTA)$_2$] and [RuClCp(PPh_3)(PTA)] were prepared as described in the literature.[56,67,93] Solvents for NMR measurements (Cortec-Euriso-top) was dried over molecular sieves (0.4 nm). ^{1}H, ^{31}P{^{1}H} NMR and ^{13}C{^{1}H} NMR spectra were recorded on a Bruker DRX300 spectrometer operating at 300.13 MHz (^{1}H), 121.49 MHz (^{31}P) and 75.47 MHz (^{13}C), respectively. Peak positions are relative to tetramethylsilane and were calibrated against the residual solvent resonance (^{1}H) or the deuterated solvent multiplet (^{13}C). Chemical shifts for ^{31}P{^{1}H} NMR were measured relative to external 85 % H_3PO_4 with downfield values taken as positive. Infrared spectra were recorded on KBr discs using an FT-IR ATI Mattson Infinity Series. Elemental analysis (C, H, N, S) was performed on a Fisons Instruments EA 1108 elemental analyser.

Synthesis of [RuCp(Adeninate–κN9)(PTA)2] (1), [RuCp(Guaninate–κN9)(PTA)2] (2) and [RuCp(Theophyllinate–κN7)(PTA)2] (3). The complexes containing two PTA ligands were obtained through the same procedure by reacting the purinate, previously obtained by reaction between the purine and KOH, and the starting complex [RuClCp(PTA)$_2$] in a mixture of EtOH/H_2O. The purine (**1**, Adenine: 18.53 mg, 0.14 mmol; **2**, Guanine: 24.22 mg, 0.16 mmol; **3**, Theophylline: 27 mg, 0.15 mmol) and KOH (**1**, **2**, **3**: 7.74 mg, 0.14 mmol) were reacted initially in 10 mL of EtOH. After 15 minutes 20 mL of H_2O were added into the resulting mixture giving rise to a colourless dissolution. After 15 minutes at room temperature the ruthenium complex [RuClCp(PTA)$_2$]) (**1**, **2**, **3**: 70.87 mg, 0.14 mmol) was added. The resulting dissolution was kept at refluxing temperature for 4 h, cooled at room temperature, filtered through sintered glass, and the solvent was removed. The resulting oil was dissolved in 2 mL of EtOH, the dissolution filtered through a sintered glass and 10 mL of Et_2O were added. The precipitated yellow powder was filtered, washed with Et_2O (2 x 2 mL) and vacuum dried.

1: Crystals useful for single crystal X-ray determination were obtained by slow recrystallization from an EtOH solution of the yellow powder obtained. Yield powder: 54.28 mg, 65 %. $S_{25,H2O}$(mg/cm^3): 15.8. Log *P*: -0.82. Elemental analysis for $C_{22}H_{33}N_{11}RuP_2$ (614,59): Found C, 42.77; H, 5.63; N, 24.87 %; calcd. C 42.99; H 5.41; N 25.07 %. IR (KBr, cm^{-1}): δ(NH_2) 1629, 1594 (s); ν(C=C+C=N) 1542 (s). ^{1}H RMN (293 K, D_2O): δ 3.89-4.9 (m, CH_2P_{PTA}, 12H); 4.49-4.87 (m, CH_2N_{PTA}, 12H); 4.82 (s, Cp, 5H); 7.66 (s, C2-H_{Ad}, 1H); 8.21 (s, C8-H_{Ad}, 1H). ^{13}C{^{1}H} RMN (293 K, D_2O): δ 55.40 (t, $^1J_{CP}$ = 8.09 Hz, NCH_2P_{PTA}); 70.59 (bs, NCH_2N_{PTA}); 78.15 (s, Cp); 119.62 (s, C5$_{Ad}$); 149.85 (s, C8$_{Ad}$); 154.07 (bs, C4$_{Ad}$); 156.54 (s, C2$_{Ad}$); 160.80 (s, C6$_{Ad}$). ^{31}P{^{1}H} RMN (293 K, D_2O): δ -23.17 (s, PTA). E = 508 mV; ΔE_p = 112 mV.

2: Yield powder: 123.83 mg, 71 %. $S_{25,H2O}$(mg/cm^3): 3.5. Log *P*: -1.19. Elemental analysis for $C_{22}H_{33}N_{11}RuP_2O$ (630.59): Found C, 41.77; H 5.43; N 24.11 %; calcd. 41.91; H 5.27; N 24.43 %. IR (KBr, cm^{-1}): δ(NH_2) 1670 (s); ν(C=O) 1625 (s); ν(C=C+C=N) 1546 (m). ^{1}H RMN (293 K, D_2O): δ 3.91-4.06 (m, CH_2N_{PTA}, 12H); 4.41-4.83 (m, CH_2P_{PTA}, 12H); 4.75 (s, Cp, 5H); 7.35 (s, C8-H_{Gu}, 1H). ^{13}C{^{1}H} RMN (293 K, D_2O): δ 55.23 (t, $^1J_{CP}$ = 7.93 Hz, NCH_2P_{PTA}); 70.63 (s, NCH_2N_{PTA}); 78.41 (s, Cp); 116.60 (s, C5$_{Gu}$); 151.37 (s, C8$_{Gu}$); 154.32 (s, C4$_{Gu}$); 159.08 (s, C2$_{Gu}$); 163.15 (s, C6$_{Gu}$). ^{31}P{^{1}H} RMN (293 K, D_2O): δ -22.78 (s, PTA). E = 768 mV; ΔE_p = 106 mV.

3: Twinned crystals were obtained by slow recrystallization from a water solution of the yellow powder. Yield powder: 171.61 mg, 82 %. $S_{25,H2O}$(mg/cm^3): 14. Log *P*: -0.45. Elemental analysis for $C_{24}H_{36}N_{10}O_2P_2Ru$ (659.63): Found C, 43.78; H 5.62; N 21.15 %; calcd. C 43.70; H 5.50; N 21.23 %. IR (KBr, cm^{-1}): ν(C$_6$=O) 1676 (s); ν(C$_2$=O) 1639 (s); ν(C=C+C=N) 1527 (m). ^{1}H RMN (293 K, D_2O): δ 3.23 (s, CH_3N1_{Tf}, 3H); 3.31 (s, CH_3N3_{Tf}, 3H); 4.10-4.95 (m, CH_2P_{PTA}, 12H); 4.93 (s, Cp, 5H); 7.16 (s, C8-H_{Tf}, 1H). ^{13}C{^{1}H} RMN (293 K, D_2O): δ 28.27 (s, CH_3N1_{Tf}); 29.84 (s, CH_3N3_{Tf}); 54.54 (bs, NCH_2P_{PTA}); 70.64 (bs, NCH_2N_{PTA}); 78.76 (s, Cp); 116.80 (s, C5$_{Tf}$); 150.10 (s, C8$_{Tf}$); 152.60 (s, C4$_{Tf}$); 154.13 (s, C2$_{Tf}$); 157.48 (s, C6$_{Tf}$). ^{31}P{^{1}H} RMN (293 K, D_2O): δ -24.21 (s, PTA). E = 590 mV; ΔE_p = 94 mV.

Synthesis of [RuCp(Adeninate–κ*N7*)(PPh_3)(PTA)] (4), [RuCp(Guaninate–κ*N7*)(PPh_3)(PTA)] (5) and [RuCp(Theophyllinate–κ*N7*)(PPh_3)(PTA)] (6). Complexes **5**, **6** and **7** were synthesized by a procedure similar to that described previously for complexes **1**, **2** and **3**, but using only EtOH as solvent. Into a 20 mL vessel was introduced the purine (**5**, Adenine: 21.00 mg, 0.15 mmol; **6**, Guanine: 25.30 mg, 0.17 mmol; **7**, Theophylline: 32 mg, 0.16 mmol), KOH (**5**, **6**, **7**: 8,00 mg, 0.14 mmol) and 10 mL of EtOH. The mixture was stirred at room temperature for 15 minutes and then complex [RuClCp(PPh_3)(PTA)]) (**5**, **6**, **7**: 80.40 mg, 0.13 mmol) was added. The mixture was refluxed for 4 h, cooled, filtered through sintered glass and concentrated to 2 mL. A yellow precipitate was obtained by addition of 5 mL of Et_2O, which was filtered, washed with Et_2O (2 x 2 mL) and vacuum dried.

4: Single crystals were obtained by slow recrystallization from an EtOH solution of the yellow powder. Yield powder: 88.68 mg, 88 %. Yield

crystals: 53.41 g, 53 %. $S_{25,H2O}$(mg/cm^3): 0.6. Log *P*: 1.4. Elemental analysis for $C_{34}H_{36}N_8P_2Ru$ (719.72): Found C, 56.82; H, 5.11; N, 15.13 %; calcd. C, 56.74; H, 5.04; N, 15.57 %. IR (KBr, cm^{-1}): $\delta(NH_2)$ 1623, 1593 (s); ν(C=C+C=N), 1541 (s). ^{1}H RMN (293 K, $CDCl_3$): δ 3.46-3.98 (m, CH_2P_{PTA}, 6H); 4.17-4.41 (m, CH_2N_{PTA}, 6H); 4.60 (s, Cp, 5H); 5.42 (bs, NH_{2Ad}, 2H); 7.20-7.56 (m, aromatic, 15H); 7.71 (s, C2-H_{Ad}, 1H); 8.34 (s, C8-H_{Ad}, 1H). ^{13}C{^{1}H} RMN (293 K, $CDCl_3$): δ 56.37 (d, $^1J_{CP}$ = 13.18 Hz, NCH_2P_{PTA}); 72.87 (d, $^1J_{CP}$ = 5.65 Hz, NCH_2N_{PTA}); 79.87 (s, Cp); 120.80 (s, $C5_{Adn}$); 128.44-133.52 (m, aromatic); 138.20 (s, $C8_{Ad}$); 149.91 (s, $C4_{Ad}$); 154.14 (s, $C2_{Ad}$); 161.86 (s, $C6_{Ad}$). ^{31}P{^{1}H} RMN (293 K, $CDCl_3$): δ -35.74 (d, $^2J_{PP}$ = 41.16 Hz, PTA); 52.12 (d, $^2J_{PP}$ = 41.16 Hz, PPh_3). E_{ox1}: 690 mV; E_{ox2} = 916 mV.

5: Yield powder: 87.40 mg, 83 %. $S_{25,H2O}$(mg/cm^3): 0.4. Log *P*: 1.32. Elemental analysis for $C_{34}H_{36}N_8P_2Ru$ (735.75): Found C, 55.60; H 5.02; N 15.09 %; calcd. C, 55.51; H 4.93; N 15.23 %. IR (KBr, cm^{-1}): $\delta(NH_2)$ 1672 (s); ν(C=O) 1608 (s); ν(C=C+C=N) 1564 (m). ^{1}H RMN (293 K, DMSO-d_6): δ 3.53-3.96 (m, CH_2P_{PTA}, 6H); 4.00-4.43 (m, CH_2N_{PTA}, 6H); 4.66 (s, Cp, 5H); 5.86 (bs, NH_{2Gu}, 2H); 7.14 (s, C8-H_{Gu}, 1H); 7.20-7.65 (m, aromatic, 15H). ^{13}C{^{1}H} RMN (293 K, DMSO-d_6): δ 55.10 (d, $^1J_{CP}$ = 15.23 Hz, NCH_2P_{PTA}); 72.56 (d, $^1J_{CP}$ = 5.70 Hz, NCH_2N_{PTA}); 80.32 (s, Cp); 118.58 (s, $C5_{Gu}$); 128.71-133.78 (m, aromatic); 151.15 (s, $C8_{Gu}$); 153.78 (s, $C4_{Gu}$); 157.68 (s, $C2_{Gu}$); 162.93 (s, $C6_{Gu}$). ^{31}P{^{1}H} RMN (293 K, DMSO-d_6): δ -39.86 (d, $^2J_{PP}$ = 40.70 Hz, PTA); 53.83 (d, $^2J_{PP}$ = 40.70 Hz, PPh_3). E = 339 mV; ΔE_p = 68 mV.

6: Yield powder: 89.92 mg, 73 %. $S_{25,H2O}$(mg/cm^3): 0.8. Log *P*: 0.81. Elemental analysis for $C_{36}H_{39}N_7O_2P_2Ru$ (764.76): Found C, 56.62; H 5.20; N 12.65 %; calcd. C, 56.54; H 5.14; N 12.82 %. IR (KBr, cm^{-1}): $\nu(C_6$=O) 1681 (s); $\nu(C_2$=O) 1628 (s); ν(C=C+C=N) 1526 (m). ^{1}H RMN (293 K, $CDCl_3$): δ 3.44-3.75 (m, CH_2N_{PTA}, 6H); 3.46 (bs, CH_3N1_{Tf}, 3H); 3.66 (bs, C**H$_3$**$N3_{Tf}$, 3H); 4.10-4.49 (m, CH_2P_{PTA}, 6H); 4.41 (s, Cp, 5H); 7.28-7.74 (m, aromatic, 15H). ^{13}C{^{1}H} RMN (293 K, $CDCl_3$): δ 28.17 (bs, CH_3N1_{Tf}); 29.77 (bs, CH_3N3_{Tf}); 55.08 (d, $^1J_{CP}$ = 12.51 Hz, NCH_2P_{PTA}); 72.83 (d, $^1J_{CP}$ = 5.84 Hz, NCH_2N_{PTA}); 80.40 (s, Cp); 117.14 (bs, $C5_{Tf}$); 127.90-133.94 (m, aromatic); 148.56 (bs, $C8_{Tf}$); 152.04 (bs, $C4_{Tf}$); 154.73 (bs, $C2_{Tf}$); 157.41 (bs, $C6_{Tf}$). ^{31}P{^{1}H} RMN (293 K, $CDCl_3$): δ -37.74 (d, $^2J_{PP}$ = 43.46 Hz, PTA); 52.36 (d, $^2J_{PP}$ = 43.46 Hz, PPh_3). E_{ox} = 726 mV.

Single crystal X-Ray diffraction. Data of compounds [RuCp(Adenine–κ*N9*)(PTA)$_2$] (**1**), [RuCp(Theophyllinate–κ*N7*)(PTA)$_2$] (**3**) and [RuCp(Adenine–κ*N7*)(PPh_3)(PTA)] (**4**) were collected on a Bruker APEX CCD diffractometer (XDIFRACT service of the University of Almería) using graphite monochromated Mo Kα radiation (λ = 0.7107 Å) at 150 K. The crystal parameters and other experimental details of the data collections for complexes **1, 3** and **4** are summarized in Table 1. Using the Olex2 software suite,[94] the structures were solved with the ShelXT[95] structure solution program using Intrinsic Phasing and refined with the ShelXL[96] refinement package using Least Squares minimisation. The data of **3** were integrated as a two components twin using SAINT. The exact twin matrix identified by the integration program was found to be -1.00007 -0.00002 0.00047, -0.87269 1.00008 -0.18402, -0.00116 0.00096 -1.00001. The absorption was corrected using Twinabs.[97] The structure was refined using the hklf 5 procedure, resulting in a BASF value of 0.5429(12). The structures have been deposited at the Cambridge Crystollagraphic Data Centre and the following deposition numbers were assigned: CCDC 1913360 (**1**), CCDC 1913362 (**3**) and CCDC 1913364 (**4**).

Growth Inhibition Assays. Cell growth inhibition assays were carried out by using the *cis*platin-sensitive T2 human cell line and the *cis*platin-resistant SKOV3 cell line for the sake of comparison with the starting complexes [RuClCp(PTA)$_2$] and [RuClCp(PPh_3)(PTA)].[55] T2 is a cell hybrid obtained by the fusion of the human lynphoblastoid line 174 (B lymphocyte transformed by the Epstein-Barr virus) with the CEM human cancer line (leukaemia T) while SKOV3 is derived from a human ovarian tumour. The cells were seeded in triplicate in 96-well trays at a density of $50{\cdot}10^3$ in 50 μl of AIM-V medium for T2, $25{\cdot}10^3$ in 50 μl of AIM-V medium for SKOV3. Stock solutions (10 mM) of the ruthenium complexes **1-6** were made in DMSO and diluted in AIM-V medium to give final concentration of 2, 10 and 50 μM. *Cis*platin was employed as a control for the *cis*platin-sensitive T2 cell line and for the *cis*platin-resistant SKOV3. Untreated cells were placed in every plate as a negative control. The cells were exposed to the compounds for 72 h and then 25 μl of a 4,5-dimethylthiozol-2-yl)2,5-diphenyltetrazolium bromide solution (12 mM) were added. After two hours of incubation, 100 μl of lysing buffer (50% DMF + 20% SDS, pH 4.7) were added to convert 4,5-dimethylthiazol-2-yl-2,5-diphenyltetrazolium bromide into a brown coloured formazane. After additional 18 hours the solution absorbance, proportional to the number of live cells, was measured by spectrophotometer and converted in % of growth inhibition.[98]

Stability Tests of the Complexes with O_2 and H_2O. The obtained ruthenium complexes were air stable for months in the solid state and for 2 days in solution. In a standard procedure, 0.01 g of **1, 2** and **3** were introduced into a 5 mm NMR tube and dissolved in 0.5 mL of D_2O. The resulting solution was cooled to 5 °C and then dry O_2 was bubbled throughout the solution for 2 min via a long syringe needle. ^{31}P{^{1}H} NMR showed that no significant changes were produced in 2 days at room temperature. No decomposition was also observed after 2 days at 40 °C as well. Additions of 50 μL of DMSO-d_6 into the complex solutions did not produce any significant change in the starting complexes after 2 days at 40 °C. A similar experiment was performed with **4**, **5** and **6** but in $CDCl_3$. These complexes showed to be stable in solution in both room temperature and 40 ºC for 2 days. Also, for these complexes additions of 50 μL of DMSO-d_6 into the solutions did not produce any significant change in the starting complexes after 2 days at 40 °C.

Stability of 2·OTf·0.25H2O first with DMSO-d6 and immediately with cell culture medium. 5 mm NMR tubes were dissolved complexes (ca. 5.4 mg) in 0,5 mL of DMSO-d_6 and then added 0.6 mL of the used cell culture medium under air. Dissolutions were studied ^{31}P{^{1}H} NMR along the time at room temperature. For all the studied complexes the results were similar, no significant changes were observed after 1 day. Similar results were obtained when solutions were kept at 40 ºC for 1 day.

Cyclic voltammetry experiments. Electrochemical experiments were performed with a VersaSTAT3 apparatus. A standard disposition for the measurement cell was used including a three-electrode glass cell consisting of a platinum disk working electrode, a platinum-wire auxiliary electrode and an Ag-metal reference electrode calibrate previously with ferrocene. The supporting electrolyte solution ($LiClO_4$, 0.05 M) was scanned over the solvent window to verify the absence of electro-active impurities. A similar concentration of the analyte (0.1 mM) in DMF was employed in all the measurements.

Octanol-Water Partition Coefficient Determination. The octanol-water partition coefficient of the ruthenium complexes was obtained by a slow-stirring method that provides accurate Log *P* results over a wide range of concentration values.[99–101] The procedure was adapted to the solubility properties of the complexes. Solutions of the complexes in the range between 10^{-4} and 10^{-3} M were prepared in octanol previously saturated with distilled water. Into a 40 mL container with a magnetic stir bar was introduced initially 10 mL of the water phase previously saturated with octanol and then by a syringe 10 mL of the octanol one so that the solution did not emulsify. The container was closed with a silicone septum and stirred slowly at 25±1 ºC. Samples were taken from the octanol and water phases with a syringe through the septum. Samples of each phase were taken periodically until the concentrations in both phases stabilized. Concentrations of the complex in each phase were measured using UV-vis spectroscopy.

Theoretical Methods. Geometry optimizations of **1**, **1a**, **4** and **4a** were run using the NWChem6.3 program package.[102] Density-functional theory (DFT) were employed at the B3LYP/def2-SVP level of theory.[103–105] For the ruthenium atom the effective core potential def2-ecp was applied. Bond energy corresponding to Ru-N7 (**1**, **4**) or Ru-N9 (**1a**, **4a**) have been obtained by subtracting the energy of the complex to the sum of the energies of the $\{RuCp(L)_2\}^+$ (L = PTA, PPh_3) and $(Adeninate)^-$ moieties, considering heterolytic cleavage of the Ru-N bond.

Table 1. Crystallographic data for **1**, **3** and **4**.

	1	**3**	**4**
Empirical formula	$C_{28}H_{53}N_{11}O_4P_2Ru$	$C_{27}H_{42}N_{10}O_3P_2Ru$	$C_{34}H_{38}N_8OP_2Ru$
Formula weight	770.82	717.71	737.73
Temperature [K]	150	150	150
Crystal system	triclinic	triclinic	monoclinic
Space group	P-1	P-1	$P2_1/c$
a [Å]	11.9945(10)	10.2996(11)	9.9148(17)
b [Å]	12.0118(10)	12.2288(12)	18.386(3)
c [Å]	13.5316(11)	12.9905(14)	17.514(3)
α [°]	110.2820(10)	81.705(2)	90
β [°]	93.2830(10)	82.803(2)	91.210(2)
γ [°]	110.4200(10)	67.685(2)	90
Volume [$Å^3$]	1678.2(2)	1493.4(3)	3192.1(9)
Z	2	2	4
ρ_{calc} [g/cm^3]	1.525	1.596	1.535
M [mm^{-1}]	0.615	0.682	0.635
F(000)	808.0	744.0	1520.0
Crystal size [mm^3]	0.06×0.04×0.02	0.5×0.3×0.2	0.04×0.03×0.02
Radiation	MoKα (λ = 0.71073)	MoKα (λ = 0.71073)	MoKα (λ = 0.71073)
Index ranges	-13 ≤ h ≤ 15 -15 ≤ k ≤ 10 -16 ≤ l ≤ 17	-12 ≤ h ≤ 13 -15 ≤ k ≤ 15 0 ≤ l ≤ 16	-12 ≤ h ≤ 12 -23 ≤ k ≤ 19 -20 ≤ l ≤ 22
Reflections collected	10304	6508	14957
Data/restraints/ parameters	6916/2/437	6508/0/393	6676/5/431
Goodness-of-fit	1.076	1.066	1.147
Final R indexes [I>=2σ (I)]	R_1 = 0.0350 wR_2 = 0.0980	R_1 = 0.0487 wR_2 = 0.1160	R_1 = 0.0942 wR_2 = 0.1698
Final R indexes [all data]	R_1 = 0.0378 wR_2 = 0.1001	R_1 = 0.0595 wR_2 = 0.1240	R_1 = 0.1281 wR_2 = 0.1888
Largest diff. peak/hole [e $Å^{-3}$]	0.85/-0.47	0.91/-0.70	0.76/-1.01

Acknowledgments

Tanks are given the European Commission FEDER program for co-financing the projects CTQ2015-67384-R (MINECO), the Junta de Andalucía PAI-research group FQM-317. Thanks are also given to A. Canella and P. Bergamini (U. Ferrara) for help with antiproliferative studies.

Keywords: antiproliferative activity, ruthenium, water, PTA, purines.

[1] B. Rosenberg, L. Van Camp, T. Krigas, *Nature* **1965**, *205*, 698–699.
[2] N. J. Farrer, L. Salassa, P. J. Sadler, *Dalt. Trans.* **2009**, *0*, 10690–10701.
[3] S. P. Foxon, T. Phillips, M. R. Gill, M. Towrie, A. W. Parker, M. Webb, J. A. Thomas, *Angew. Chemie - Int. Ed.* **2007**, *46*, 3686–3688.
[4] A. Neves, M. Lanznaster, A. J. Bortoluzzi, R. A. Peralta, A. Casellato, E. E. Castellano, P. Herrald, M. J. Riley, G. Schenk, *J. Am. Chem. Soc.* **2007**, *129*, 7486–7487.
[5] C. Metcalfe, J. A. Thomas, *Chem. Soc. Rev.* **2003**, *32*, 215–224.
[6] M. J. Clarke, F. Zhu, D. R. Frasca, *Chem. Rev.* **2002**, *99*, 2511–2534.
[7] B. M. Zeglis, V. C. Pierre, J. K. Barton, *Chem. Commun.* **2007**, *0*, 4565–4579.
[8] J. Reedijk, *Proc. Natl. Acad. Sci.* **2003**, *100*, 3611–3616.
[9] G. Mestroni, E. Alessio, G. Sava, S. Pacor, M. Coluccia, A. Boccarelli, *Met. Based. Drugs* **2007**, *1*, 41–63.
[10] M. Coluccia, G. Sava, F. Loseto, A. Nassi, A. Boccarelli, D. Giordano, E. Alessio, G. Mestroni, *Eur. J. Cancer* **1993**, *29A*, 1873–9.
[11] B. Stordal, M. Davey, *IUBMB Life* **2007**, *59*, 696–699.
[12] J. Reedijk, *Platin. Met. Rev.* **2008**, *52*, 2–11.
[13] F. Marchetti, R. Pettinari, C. Di Nicola, C. Pettinari, J. Palmucci, R. Scopelliti, T. Riedel, B. Therrien, A. Galindo, P. J. Dyson, *Dalt. Trans.* **2018**, *47*, 868–878.
[14] C. Gaiddon, M. Pfeffer, *Eur. J. Inorg. Chem.* **2017**, *2017*, 1639–1654.
[15] S. Q. Yap, C. F. Chin, A. H. Hong Thng, Y. Y. Pang, H. K. Ho, W. H. Ang, *ChemMedChem* **2017**, *12*, 300–311.
[16] J. Palmucci, F. Marchetti, R. Pettinari, C. Pettinari, R. Scopelliti, T. Riedel, B. Therrien, A. Galindo, P. J. Dyson, *Inorg. Chem.* **2016**, *55*, 11770–11781.
[17] C. Ríos-Luci, L. G. León, A. Mena-Cruz, E. Pérez-Roth, P. Lorenzo-Luis, A. Romerosa, J. M. Padrón, *Bioorganic Med. Chem. Lett.* **2011**, *21*, 4568–4571.
[18] E. R. Jamieson, S. J. Lippard, *Chem. Rev.* **1999**, *99*, 2467–2498.
[19] E. Alessio, Z. Guo, *Eur. J. Inorg. Chem.* **2017**, *2017*, 1539–1540.
[20] E. Alessio, *Eur. J. Inorg. Chem.* **2017**, *2017*, 1549–1560.
[21] P. Zhang, P. J. Sadler, *Eur. J. Inorg. Chem.* **2017**, *2017*, 1541–1548.
[22] I. Romero-Canelón, P. J. Sadler, *Inorg. Chem.* **2013**, *52*, 12276–12291.
[23] K. Laws, G. Bineva-Todd, A. Eskandari, C. Lu, N. O'Reilly, K. Suntharalingam, *Angew. Chemie Int. Ed.* **2018**, *57*, 287–291.
[24] X.-Q. Zhou, A. Busemann, M. S. Meijer, M. A. Siegler, S. Bonnet, *Chem. Commun.* **2019**, *55*, 4695–4698.
[25] D. Armstrong, S. M. Kirk, C. Murphy, A. Guerriero, M. Peruzzini, L. Gonsalvi, A. D. Phillips, *Inorg. Chem.* **2018**, *57*, 6309–6323.
[26] L. Biancalana, L. K. Batchelor, G. Ciancaleoni, S. Zacchini, G. Pampaloni, P. J. Dyson, F. Marchetti, *Dalt. Trans.* **2018**, *47*, 9367–9384.
[27] A. G. Quiroga, C. Navarro Ranninger, *Coord. Chem. Rev.* **2004**, *248*, 119–133.
[28] J. Furrer, G. Süss-Fink, *Coord. Chem. Rev.* **2016**, *309*, 36–50.
[29] W. M. Motswainyana, P. A. Ajibade, *Adv. Chem.* **2015**, *2015*, 1–21.
[30] S. Betanzos-Lara, L. Salassa, A. Habtemariam, P. J. Sadler, *Chem. Commun.* **2009**, *0*, 6622–6624.
[31] G. I. Pascu, A. C. G. Hotze, C. Sanchez-Cano, B. M. Kariuki, M. J. Hannon, *Angew. Chemie Int. Ed.* **2007**, *46*, 4374–4378.
[32] H. A. Wee, P. J. Dyson, *Eur. J. Inorg. Chem.* **2006**, *2006*, 4003–4018.
[33] Y. K. Yan, M. Melchart, A. Habtemariam, P. J. Sadler, *Chem. Commun.* **2005**, *0*, 4764–4776.
[34] A. C. G. Hotze, S. E. Caspers, D. De Vos, H. Kooijman, A. L. Spek, A. Flamigni, M. Bacac, G. Sava, J. G. Haasnoot, J. Reedijk, *J. Biol. Inorg. Chem.* **2004**, *9*, 354–364.
[35] W. H. Ang, A. Casini, G. Sava, P. J. Dyson, *J. Organomet. Chem.* **2011**, *696*, 989–998.
[36] G. Süss-Fink, *Dalt. Trans.* **2010**, *39*, 1673–1688.
[37] E. Alessio, G. Mestroni, A. Bergamo, G. Sava, *Curr. Top. Med. Chem.* **2004**, *4*, 1525–35.
[38] E. Alessio, G. Mestroni, A. Bergamo, G. Sava, *Met. Ions Biol. Syst.* **2004**, *42*, 323–351.
[39] B. S. Murray, M. V. Babak, C. G. Hartinger, P. J. Dyson, *Coord. Chem. Rev.* **2016**, *306*, 86–114.
[40] A. Bergamo, P. J. Dyson, G. Sava, *Coord. Chem. Rev.* **2018**, *360*, 17–33.
[41] K. Jeyalakshmi, J. Haribabu, C. Balachandran, S. Swaminathan, N. S. P. Bhuvanesh, R. Karvembu, *Organometallics* **2019**, *38*, 753–770.
[42] S. Thota, D. A. Rodrigues, D. C. Crans, E. J. Barreiro, *J. Med. Chem.* **2018**, *61*, 5805–5821.
[43] C. G. Hartinger, S. Zorbas-Seifried, M. A. Jakupec, B. Kynast, H. Zorbas, B. K. Keppler, *J. Inorg. Biochem.* **2006**, *100*, 891–904.
[44] L. Biancalana, G. Pampaloni, F. Marchetti, *Chimia (Aarau).* **2017**, *71*, 573–579.
[45] L. Biancalana, I. Abdalghani, F. Chiellini, S. Zacchini, G. Pampaloni, M. Crucianelli, F. Marchetti, *Eur. J. Inorg. Chem.* **2018**, *2018*, 3041–3057.
[46] J. Furrer, G. Süss-Fink, *Coord. Chem. Rev.* **2016**, *309*, 36–50.
[47] P. Zhang, P. J. Sadler, *J. Organomet. Chem.* **2017**, *839*, 5–14.
[48] A. Guerriero, M. Peruzzini, L. Gonsalvi, *Coord. Chem. Rev.* **2018**, *355*, 328–361.
[49] J. Bravo, S. Bolaño, L. Gonsalvi, M. Peruzzini, *Coord. Chem. Rev.* **2010**, *254*, 555–607.
[50] A. D. Phillips, L. Gonsalvi, A. Romerosa, F. Vizza, M. Peruzzini, *Coord. Chem. Rev.* **2004**, *248*, 955–993.
[51] F. Scalambra, P. Lorenzo-Luis, I. de los Ríos, A. Romerosa, *Eur. J. Inorg. Chem.* **2019**, *2019*, 1529–1538.
[52] A. Wołoszyn, C. Pettinari, R. Pettinari, G. V. Badillo Patzmay, A. Kwiecień, G. Lupidi, M. Nabissi, G. Santoni, P. Smoleński, *Dalt. Trans.* **2017**, *46*, 10073–10081.
[53] L. Côrte-Real, R. G. Teixeira, P. Gírio, E. Comsa, A. Moreno, R. Nasr, H. Baubichon-Cortay, F. Avecilla, F. Marques, M. P. Robalo, et al., *Inorg. Chem.* **2018**, *57*, 4629–4639.
[54] A. Romerosa, P. Bergamini, V. Bertolasi, A. Canella, M. Cattabriga, R. Gavioli, S. Mañas, N. Mantovani, L. Pellacani, *Inorg. Chem.* **2004**, *43*, 905–913.
[55] P. Bergamini, V. Bertolasi, L. Marvelli, A. Canella, R. Gavioli, N. Mantovani, S. Mañas, A. Romerosa, *Inorg. Chem.* **2007**, *46*, 4267–

4276.
[56] A. Romerosa, T. Campos-Malpartida, C. Lidrissi, M. Saoud, M. Serrano-Ruiz, M. Peruzzini, J. A. Garrido-Cárdenas, F. García-Maroto, *Inorg. Chem.* **2006**, *45*, 1289–1298.
[57] A. Mena-Cruz, P. Lorenzo-Luis, A. Romerosa, M. Saoud, M. Serrano-Ruiz, *Inorg. Chem.* **2007**, *46*, 6120–6128.
[58] A. Mena-Cruz, P. Lorenzo-Luis, A. Romerosa, M. Serrano-Ruiz, *Inorg. Chem.* **2008**, *47*, 2246–2248.
[59] A. Mena-Cruz, P. Lorenzo-Luis, V. Passarelli, A. Romerosa, M. Serrano-Ruiz, *Dalt. Trans.* **2011**, *40*, 3237–3244.
[60] A. Mena-Cruz, M. Serrano-Ruiz, P. Lorenzo-Luis, A. Romerosa, Á. Kathó, F. Joó, L. M. Aguilera-Sáez, *J. Mol. Catal. A Chem.* **2016**, *411*, 27–33.
[61] M. Serrano-Ruiz, L. M. Aguilera-Sáez, P. Lorenzo-Luis, J. M. Padrón, A. Romerosa, *Dalt. Trans.* **2013**, *42*, 11212–11219.
[62] Z. Mendoza, P. Lorenzo-Luis, M. Serrano-Ruiz, E. Martín-Batista, J. M. Padrón, F. Scalambra, A. Romerosa, *Inorg. Chem.* **2016**, *55*, 7820–7822.
[63] Z. Mendoza, P. Lorenzo-Luis, F. Scalambra, J. M. Padrón, A. Romerosa, *Dalt. Trans.* **2017**, *46*, 8009–8012.
[64] Z. Mendoza, P. Lorenzo-Luis, F. Scalambra, J. M. Padrón, A. Romerosa, *Eur. J. Inorg. Chem.* **2018**, *2018*, 4660–4660.
[65] L. Hajji, C. Saraiba-Bello, A. Romerosa, G. Segovia-Torrente, M. Serrano-Ruiz, P. Bergamini, A. Canella, *Inorg. Chem.* **2011**, *50*, 873–882.
[66] L. Hajii, C. Saraiba Bello, F. Scalambra, G. Segovia-Torrente, A. Romerosa, A. Canella, *J. Coord. Chem.* **2017**, *70*, 1632–1644.
[67] D. N. Akbayeva, L. Gonsalvi, W. Oberhauser, M. Peruzzini, F. Vizza, P. Brüggeller, A. Romerosa, G. Sava, A. Bergamo, *Chem. Commun.* **2003**, *0*, 264–265.
[68] M. S. Rahman, H. Q. Yuan, T. Kikuchi, I. Fujisawa, K. Aoki, *J. Mol. Struct.* **2010**, *966*, 92–101.
[69] H.-F. Ma, Q.-Y. Liu, Y.-L. Wang, S.-G. Yin, *Inorg. Chem.* **2017**, *56*, 2919–2925.
[70] E. Colacio, A. Romerosa, J. Ruiz, P. Román, J. M. Gutiérrez-Zorrilla, M. Martínez-Ripoll, *J. Chem. Soc., Dalt. Trans.* **1989**, *0*, 2323–2329.
[71] "The Cambridge Crystallographic Data Centre (CCDC)," can be found under https://www.ccdc.cam.ac.uk/, **n.d.**
[72] H. Bougherra, O. Berradj, A. Adkhis, *J. Chem. Pharm. Res.* **2018**, *10*, 93–103.
[73] Y. Kou, M.-C. Koag, S. Lee, *Biochemistry* **2018**, *57*, 5105–5116.
[74] Y. Zhang, C. Liu, F. Wang, Z. Liu, J. Ren, X. Qu, *Chem. Commun.* **2017**, *53*, 1840–1843.
[75] A. Szadkowska, S. Staszko, E. Zaorska, R. Pawłowski, *RSC Adv.* **2016**, *6*, 44248–44253.
[76] S. A. Shaker, *E-Journal Chem.* **2011**, *8*, 153–158.
[77] A. Romerosa, C. López-Magaña, M. Saoud, S. Mañas, E. Colacio, J. Suárez-Varela, *Inorganica Chim. Acta* **2000**, *307*, 125–130.
[78] W. S. Sheldrick, C. Landgrafe, *Inorganica Chim. Acta* **1993**, *208*, 145–151.
[79] S. Korn, W. S. Sheldrick, *J. Chem. Soc. Dalt. Trans.* **1997**, *0*, 2191–2200.
[80] S. Korn, W. S. Sheldrick, *Inorganica Chim. Acta* **1997**, *254*, 85–91.
[81] W. M. Beck, N. D. Kottmair, J. C. Calabrese, *Inorg. Chem.* **1979**, *18*, 176–182.
[82] K. Aoki, M. A. Salam, C. Munakata, I. Fujisawa, *Inorganica Chim. Acta* **2007**, *360*, 3658–3670.
[83] K. D. Klika, H. Kivelä, V. V. Ovcharenko, V. Nieminen, R. Sillanpää, J. Arpalahti, *Dalt. Trans.* **2007**, *0*, 3966–3970.
[84] A. C. Morel, D. Choquesillo-Lazarte, C. Alarcón-Payer, J. M. González-Pérez, A. Castiñeiras, J. Niclós-Gutiérrez, *Inorg. Chem. Commun.* **2003**, *6*, 1354–1357.
[85] K. Krogh-Jespersen, R. T. Stibrany, E. John, J. D. Westbrook, T. J. Emge, M. J. Clarke, J. A. Potenza, H. J. Schugar, *Inorg. Chem.* **2008**, *47*, 9813–9827.
[86] T. J. Kistenmacher, D. J. Szalda, L. G. Marzilli, *Inorg. Chem.* **1975**, *14*, 1686–1691.
[87] E. Buncel, R. Kumar, A. R. Norris, A. L. Beauchamp, *Can. J. Chem.* **2006**, *63*, 2575–2581.
[88] A. A. Norris, S. E. Taylor, E. Buncel, F. Bélanger-Gariépy, A. L. Beauchamp, *Inorganica Chim. Acta* **1984**, *92*, 271–274.
[89] K. Caldwell, G. B. Deacon, B. M. Gatehouse, S. C. Lee, A. J. Canty, *Acta Crystallogr. Sect. C Cryst. Struct. Commun.* **2002**, *40*, 1533–1536.
[90] T. J. Kistenmacher, *Acta Crystallogr. Sect. B Struct. Crystallogr. Cryst. Chem.* **2002**, *31*, 85–89.
[91] M. J. Gardner, R. X. Smith, E. Shefter, *J. Pharm. Sci.* **1983**, *72*, 348–350.
[92] D. D. Perrin, W. L. F. Armarego, D. R. Perrin, *The Purification of Laboratory Chemicals*, Elsevier/BH, **1980**.
[93] D. J. Daigle, T. J. Decuir, J. B. Robertson, D. J. Darensbourg, *Inorg. Synth.* **2007**, *32*, 40–45.
[94] O. V. Dolomanov, L. J. Bourhis, R. J. Gildea, J. A. K. Howard, H. Puschmann, IUCr, *J. Appl. Crystallogr.* **2009**, *42*, 339–341.
[95] G. M. Sheldrick, *Acta Crystallogr. Sect. A Found. Crystallogr.* **2015**, *71*, 3–8.
[96] G. M. Sheldrick, *Acta Crystallogr. Sect. C, Struct. Chem.* **2015**, *71*, 3–8.
[97] Bruker AXS Inc, **2008**.
[98] M. B. Hansen, S. E. Nielsen, K. Berg, *J. Immunol. Methods* **1989**, *119*, 203–210.
[99] H. R. Lozano, F. Martínez, *Brazilian J. Pharm. Sci.* **2006**, 601–613.
[100] L. Ropel, L. S. Belvèze, S. N. V. K. Aki, M. A. Stadtherr, J. F. Brennecke, *Green Chem.* **2005**, *7*, 83–90.
[101] R. Mannhold, G. I. Poda, C. Ostermann, I. V. Tetko, *J. Pharm. Sci.* **2009**, *98*, 861–893.
[102] M. Valiev, E. J. Bylaska, N. Govind, K. Kowalski, T. P. Straatsma, H. J. J. Van Dam, D. Wang, J. Nieplocha, E. Apra, T. L. Windus, et al., *Comput. Phys. Commun.* **2010**, *181*, 1477–1489.
[103] A. D. Becke, *J. Chem. Phys.* **1993**, *98*, 1372–1377.
[104] C. Lee, W. Yang, R. G. Parr, *Phys. Rev. B* **1988**, *37*, 785–789.
[105] F. Weigend, R. Ahlrichs, *Phys. Chem. Chem. Phys.* **2005**, *7*, 3297–3305.